Visualization of nonlinear effects in reflecting internal wave beams

Thomas Peacock and Ali Tabaei
Department of Mechanical Engineering, Massachusetts Institute of Technology, Cambridge, Massachusetts 02139

(Received 9 March 2005; accepted 25 April 2005; published online 27 May 2005)

Recent theoretical and numerical investigations predict that localized nonlinear effects in the overlapping region of an incoming and reflected internal wave beam can radiate higher-harmonic beams. We present the first set of experimental visualizations, obtained using the digital Schlieren method, that confirm the existence of radiated higher-harmonic beams. For arrangements in which the angle of propagation of the second harmonic exceeds the slope angle, radiated beams are visualized. When the propagation angle of the second harmonic deceeds the slope angle no radiated beams are detected, as the associated density gradient perturbations are too weak for the experimental method. The case of a critical slope is also reported. © *2005 American Institute of Physics*. [DOI: 10.1063/1.1932309]

The reflection of internal gravity waves from topography plays an important role in ocean dynamics.[1–3] These waves reflect off a boundary in such a manner that the angle of propagation with respect to the direction of gravity is conserved, not the angle with respect to the boundary normal, which is the case in acoustics or optics. This nonintuitive property is a consequence of the dispersion relation for a uniformly stratified Boussinesq fluid, which in the absence of background rotation may be written as

$$\frac{\omega}{N} = \sin\theta, \tag{1}$$

with θ being the angle the phase velocity makes with gravity, and ω and N the excitation and buoyancy frequencies, respectively. Since the frequency of the waves is preserved upon reflection, so is θ. Furthermore, for internal gravity waves phase and group velocity are perpendicular, making θ also the angle of energy propagation with respect to level surfaces. The presence of background rotation, such as exists in the ocean, modifies the dispersion relation (1), reducing θ for a given ω and N.[4]

Nonlinear planar internal waves of frequency ω, propagating at angle θ with respect to the horizontal, generate higher harmonics when reflected from a slope of angle α.[5] Much interest has been placed on the near critical case $\theta \sim \alpha$, which has been identified as an important scenario for generating mixing, either through overturning or shear-flow instability.[6–9] In the particular case of an incident wave beam originating from a localized source, the higher harmonics and associated mixing have been studied in the confined overlap region of the incoming and reflected wave beams.[10–13]

Recent theoretical and numerical investigations predict that localized nonlinear effects in the overlapping region of an incoming and reflected wave beam can also radiate higher-harmonic beams.[14,15] Specifically, a primary-harmonic beam of frequency ω_1 propagating at angle θ_1 to the horizontal and incident on a slope of angle α yields a reflected wave beam of the same frequency, which propagates up-slope or down-slope depending on whether $\theta_1 > \alpha$ or $\theta_1 < \alpha$, respectively. Nonlinearity induces harmonics in the overlapping region of the incoming and reflected beams, turning this region into a source of new beams, provided that the frequency of the induced harmonics $\omega_n = n\omega < N$, n being the order of the harmonic. The new beams propagate up-slope or down-slope, depending on whether their angle of propagation $\theta_n = \sin^{-1}(\omega_n/N)$ exceeds or deceeds α, respectively. In previous numerical[11,16] and experimental studies,[10,12,17] radiated beams were not observed either because $\omega_n > N$ or the study was confined to the region of interaction.

The goal of this study is to obtain the first experimental evidence of radiated higher-harmonic beams arising from the interaction of an incident and reflected primary-harmonic beam. The experimental apparatus comprised an acrylic tank 1.28 m long, 0.66 m high, and 0.2 m wide, with walls 3/4 in. thick. The tank was filled from below with salt water and stratified using the Oster double bucket method.[18] A Precision Measurement Engineering (PME) fast conductivity and temperature probe, mounted on a linear traverse, was used to measure the stratification. The probe was calibrated using an Anton–Paar densitometer accurate to $0.002\,\mathrm{kg/m^3}$ and 0.1 °C, and oriented parallel to gravity using a plumbline. The resulting density gradients were found to be highly linear, but varied slightly in magnitude between experiments due to the effect of different arrangements of inclined walls and antireflection barriers on the filling process. The magnitude of the density gradient was also inferred by using radon transform techniques to measure the angle of propagation of a wave beam for a given forcing frequency.[4]

A wave beam was generated by replacing the salinity probe mounted on the linear traverse with a thin aluminum support rod, onto the end of which was affixed an acrylic cylinder 12.5 mm in diameter and 0.195 m long. A schematic of the arrangement is shown in Fig. 1. The cylinder, which extended the width of the tank save for a 2.5 mm gap between both the front and back walls of the tank, was lowered slowly to a desired point in the stratification and left to settle

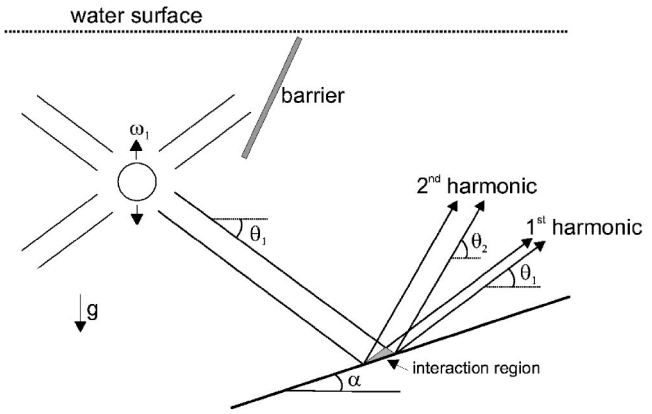

FIG. 1. Schematic of the experimental arrangement.

for several minutes. A large amplitude sinusoidal oscillation, with a peak-to-peak displacement of 15.0 mm, was then used to generate nonlinear wave beams. The sinusoidal motion of the cylinder, driven by a Labview motion control system, generated four wave beams (the celebrated St-Andrews' cross). Three of the beams were blocked using appropriately placed barriers, while one beam was free to propagate. The free beam reflected from an inclined boundary that extended the width of the tank, save for a 2.5 mm gap between both the front and back walls to allow passage of water during filling, and the emerging wave beams were studied.

The wave beams were visualized using the digital Schlieren method.[19] A random pattern of dots, printed on a transparency and backlit by an electroluminescent screen, were placed behind the tank. The backlit pattern was viewed through the tank using a JAI CV-M4+CL CCD camera with a resolution of 1268×1024 pixels, running in 8-bit mode. As viewed by the camera, the random pattern appeared distorted by the wave motion in the incoming and reflected wave beams, which were assumed uniform across the width of the tank. The apparent displacements of the pattern, which are related to the perturbation of the local density gradient, were detected and rendered visible by the software Digiflow.

The first set of visualizations, presented in Fig. 2, concern an incoming primary-harmonic beam propagating at $\theta_1=24.8°\pm0.2°$ to the horizontal, generated by oscillating the cylinder with frequency $\omega_1=0.536$ rad/s in a stratification of buoyancy frequency $N=1.28\pm0.03$ rad/s. Here, the buoyancy frequency has been calculated using the local density at the cylinder level and the variability in N is an indication of its smooth variation due to the linear, rather than exponential, density profile in the tank. We present a sequence of images recorded at three different stages in the evolution of the wave beam reflected from a slope with inclination $\alpha=15.0\pm0.1°$. The images, for which the oscillating cylinder is positioned beyond the left-hand boundary, were taken 49 s, 85 s, and 146 s after the commencement of oscillation. Intensities in each image are related to the local horizontal density gradient, which exists solely due to perturbation of the ambient stratification by the wave beams. For small-amplitude waves the relation is linear,[19] but for nonlinear disturbances this is not necessarily so. We have not

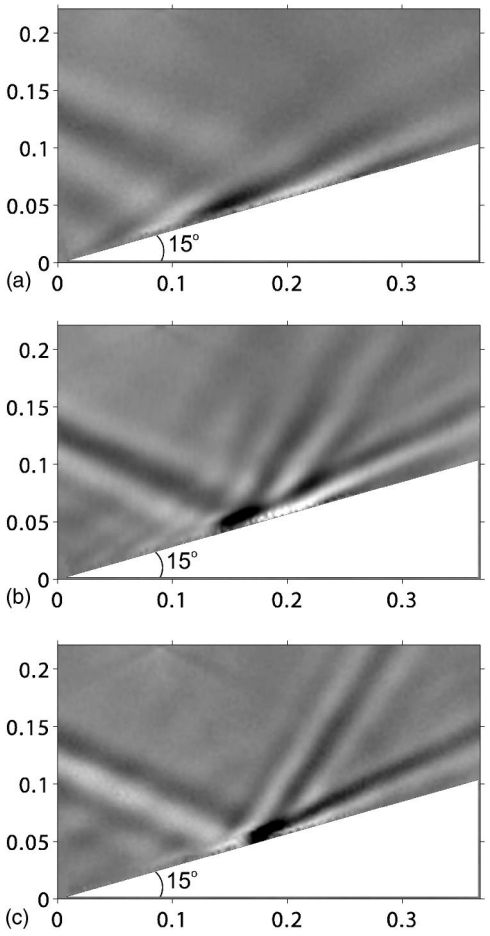

FIG. 2. Images of reflection of a primary-harmonic wave beam for $\theta_2>\theta_1>\alpha$. (a) 49 s, (b) 85 s, (c) 146 s. Length scale in meters.

yet quantified the relationship for these visualizations; this is the subject of future investigations. For consistency, however, the length scales, physical parameters, and saturation levels used in processing were coordinated so that pixel intensity had the same meaning for all visualizations presented in this Letter.

In Fig. 2(a) there is noticeable spreading of the incoming primary-harmonic beam due to transients from the start up of the cylinder. The reflected primary-harmonic beam propagates up-slope, since $\theta_1>\alpha$. In Fig. 2(b) the incoming primary-harmonic beam has become quite uniform along its length, although there is slight spreading due to viscous effects,[20] and the emergence of a second-harmonic beam can be seen. The angle of propagation with respect to the horizontal for the second-harmonic beam is $\theta_2=58.0\pm0.2°$, consistent with the dispersion relation (1) for a beam of frequency $\omega_2=2\omega_1$. The second-harmonic beam also propagates up-slope, since $\theta_2>\alpha$. Notably, the second-harmonic beam took significantly longer to establish than the reflected primary-harmonic beam. In part, we attribute this delay to the lower group velocity of second-harmonic waves compared to primary-harmonic waves; transient effects in the interaction region of the incident and reflected primary-harmonic beams also played a role, however. Finally, in Fig.

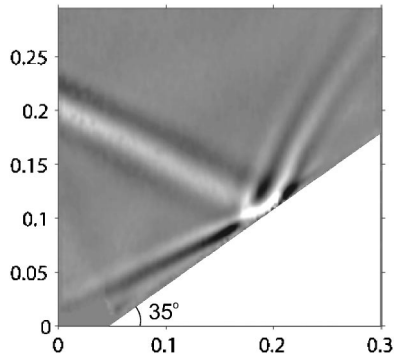

FIG. 3. Image of reflection of a primary-harmonic wave beam for $\theta_2 > \alpha > \theta_1$. Length scale in meters.

2(c), the radiated second-harmonic beam is fully established and has achieved a steady state.

The visualization of a wave beam propagating at an angle of $\theta_1 = 27.7° \pm 0.2°$ and reflected from a slope of inclination $\alpha = 35.0° \pm 0.1°$ is presented in Fig. 3. The incoming beam from the upper left corner was generated by oscillating the cylinder with frequency $\omega_1 = 0.538$ rad/s in a stratification $N = 1.16 \pm 0.03$ rad/s. In this arrangement, the wave beams emanating from the interaction region are divided by the slope: the primary-harmonic beam is forced down-slope, since $\theta_1 < \alpha$; the second-harmonic beam travels up-slope, since $\theta_2 > \alpha$. Again, the radiated second-harmonic beam took significantly longer to establish than the reflected primary-harmonic beam, achieving a steady state by the time this image was taken, 120 s after the cylinder began oscillating.

The case of a primary-harmonic wave beam propagating at angle $23.9° \pm 0.2°$ and reflected from a slope with $\alpha = 65.0° \pm 0.1°$ is presented in Fig. 4. The incoming wave beam was generated by oscillating the cylinder at a frequency $\omega_1 = 0.506$ rad/s in a stratification of buoyancy frequency $N = 1.24 \pm 0.03$ rad/s. Since $\theta_1 < \theta_2 < \alpha$, both outgoing beams must propagate down-slope in this arrangement. Although the reflected primary-harmonic beam can be clearly seen in Fig. 4, there is no evidence of a radiated second-harmonic beam from the interaction region (only a weak second-harmonic beam generated by the oscillating cylinder can be seen in the lower left corner of the image). The absence of the second harmonic in our visualization is

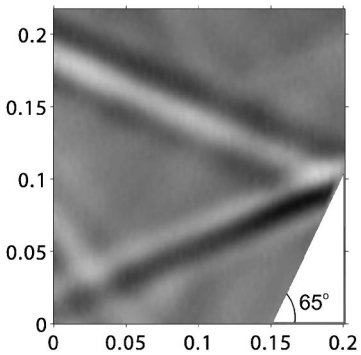

FIG. 4. Image of reflection of a primary-harmonic wave beam for $\alpha > \theta_2 > \theta_1$. Length scale in meters.

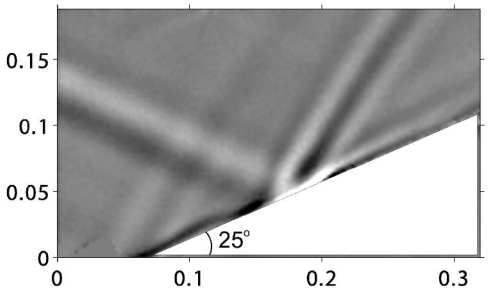

FIG. 5. Image of reflection of a primary-harmonic wave beam for $\theta_2 > \theta_1 = \alpha$. Length scale in meters.

consistent with numerical calculations for inviscid wave beam reflection, which predict that the energy radiated as a second harmonic for $\alpha = 65°$ is less than 1% of that for $\alpha = 35°$;[15] in this case, our digital Schlieren system does not have the required sensitivity to resolve the associated density gradient perturbations.

Finally, we investigated the critical case $\theta = \alpha$, which has been the subject of much investigation.[9,13,21] An incoming beam at an angle $\theta_1 = 25.1° \pm 0.2°$, generated by oscillating the cylinder at frequency $\omega_1 = 0.503$ rad/s in a stratification with $N = 1.19 \pm 0.3$ rad/s, was reflected from a slope of angle $\alpha = 25.0° \pm 0.1°$. The visualization after 182 s is shown in Fig. 5. In this case there is no reflected primary harmonic, as the direction of propagation is aligned with the slope, but a clear second-harmonic beam exists with a propagation angle of $\theta_2 = 58.3° \pm 0.2°$. We also note that a weak second-harmonic beam, originating from the oscillating cylinder and reflected from a lower boundary in the tank, can be seen emanating from the bottom left corner of the image. For this arrangement, inviscid theory predicts that there is no steady-state solution and the second harmonic originating from the interaction region grows linearly with time, ultimately leading to an overturning of the density field;[8,12,20] we observed no such overturning in our experiments. Accounting for viscosity, however, enables a steady-state solution to be found,[9,21] and this is what we observed experimentally.

In conclusion, we have presented the first experimental evidence for the existence of radiated second-harmonic internal wave beams, generated by the localized nonlinear interaction between an incident and reflected primary-harmonic wave beam. This phenomenon can occur in the oceans wherever wave beams are reflected, from bathymetry or the thermocline, for example. Given the low angle of beam propagation in the oceans, such an interaction would generate many higher harmonics; the energy of the incoming beam being distributed among several outgoing beams. Finally, we remark that this mechanism will also affect the nature of attractors for nonlinear internal waves in a confined stably stratified fluid,[22] drawing energy from the first-harmonic attractor to higher harmonics.

This work was supported in part by the AFOSR, AFMC, USAF under Grant No. F49620-01-1-001, and by the NSF Grant No. DMS-0305940. The authors acknowledge helpful interactions with T. Akylas and S. Dalziel, and assistance in image processing from P. Echeverri.

[1]C. C. Ericksen, "Internal wave reflection and mixing at Fieberling Guyot," J. Geophys. Res. **103**, 2977 (1998).
[2]C. Garrett and D. Gilbert, "Estimates of vertical mixing by internal waves reflected off sloping topography," in *Small-Scale Turbulence and Mixing in the Ocean*, edited by J. C. J. Nihoul and B. M. Janard (Elsevier Scientific, New York, 1988).
[3]L. St. Laurent and C. Garrett, "The role of internal tides in mixing in the deep ocean," J. Phys. Oceanogr. **32**, 2882 (2002).
[4]T. Peacock and P. D. Weidman, "The effect of rotation on conical wave beams," Exp. Fluids (to be published).
[5]S. A. Thorpe, "On the reflection of a train of finite amplitude internal waves from a uniform slope," J. Fluid Mech. **178**, 279 (1987); S. A. Thorpe and A. P. Haines, "A note on obesrvations of wave reflection on a 20° slope," Appendix C in J. Fluid Mech. article by Thorpe.
[6]D. R. Cacchione and C. Wunsch, "Experimental study of internal waves over a slope," J. Fluid Mech. **66**, 223 (1974).
[7]G. N. Ivey and R. I. Nokes, "Vertical mixing due to breaking of critical internal waves on sloping boundaries," J. Fluid Mech. **204**, 479 (1989).
[8]D. N. Slinn and J. J. Riley, "Turbulent dynamics of a critically reflecting internal gravity wave," Theor. Comput. Fluid Dyn. **11**, 281 (1998).
[9]T. Dauxois and W. R. Young, "Near-critical reflection of internal waves," J. Fluid Mech. **390**, 271 (1999).
[10]I. P. D. DeSilva, J. Imberger, and G. N. Ivey, "Localized mixing due to a breaking internal wave ray at a sloping bed," J. Fluid Mech. **350**, 1 (1997).
[11]A. Javam, J. Imberger, and S. W. Armfield, "Numerical study of internal wave reflection from sloping boundaries," J. Fluid Mech. **396**, 183 (1999).
[12]G. N. Ivey, K. B. Winters, and I. P. D. Desilva, "Turbulent mixing in a sloping benthic boundary layer energized by internal waves," J. Fluid Mech. **418**, 59 (2000).
[13]T. Dauxois, A. Didier, and E. Falcon, "Observation of near-critical reflection of internal waves in a stably stratified fluid," Phys. Fluids **16**, 1936 (2004).
[14]K. G. Lamb, "Nonlinear interaction among internal wave beams generated by tidal flow over supercritical topography," Geophys. Res. Lett. **31**, L09313 (2004).
[15]A. Tabaei, T. R. Akylas and K. G. Lamb, "Nonlinear effects in reflecting and colliding internal wave beams," J. Fluid Mech. **526**, 217 (2005).
[16]A. Javam, J. Imberger, and S. W. Armfield, "Numerical study of internal wave-wave interactions in a stratified fluid, " J. Fluid Mech. **415**, 65 (2000).
[17]S. G. Teoh, G. N. Ivey and J. Imberger, "Laboratory study of the interaction between two internal wave rays," J. Fluid Mech. **336**, 91 (1997).
[18]G. Oster, "Density gradients," Sci. Am. **213**, 70 (1965).
[19]B. R. Sutherland, S. B. Dalziel, G. O. Hughes, and P. F. Linden, "Visualisation and measurement of internal waves by synthetic schlieren. Part 1: Vertically oscillating cylinder," J. Fluid Mech. **390**, 93 (1999).
[20]N. H. Thomas and T. N. Stevenson, "A similarity solution for viscous internal waves," J. Fluid Mech. **54**, 495 (1972).
[21]A. Tabaei, "Theoretical and experimental study of nonlinear internal gravity wave beams," Ph.D. thesis, Department of Civil and Environmental Engineering, Massachusetts Institute of Technology, 2005.
[22]L. R. M. Maas, D. Benielli, J. Sommeria, and F. P. A. Lam, "Observation of an internal wave attractor in a confined, stably stratified fluid," Nature (London) **388**, 557 (1997).